Forcing a Distributed Glacier Mass Balance Model with the Regional Climate Model REMO. Part I: Climate Model Evaluation

SVEN KOTLARSKI*

Max Planck Institute for Meteorology, Hamburg, Germany

FRANK PAUL

Department of Geography, University of Zurich, Zurich, Switzerland

DANIELA JACOB

Max Planck Institute for Meteorology, Hamburg, Germany

(Manuscript received 7 July 2008, in final form 13 July 2009)

ABSTRACT

A coupling interface between the regional climate model REMO and a distributed glacier mass balance model is presented in a series of two papers. The first part describes and evaluates the reanalysis-driven regional climate simulation that is used to force a mass balance model for two glaciers of the Swiss mass balance network. The detailed validation of near-surface air temperature, precipitation, and global radiation for the European Alps shows that the basic spatial and temporal patterns of all three parameters are reproduced by REMO. Compared to the Climatic Research Unit (CRU) dataset, the Alpine mean temperature is underestimated by 0.34°C. Annual precipitation shows a positive bias of 17% (30%) with respect to the uncorrected gridded ALP-IMP (CRU) dataset. A number of important and systematic model biases arise in high-elevation regions, namely, a negative temperature bias in winter, a bias of seasonal precipitation (positive or negative, depending on gridbox altitude and season), and an underestimation of springtime and overestimation of summertime global radiation. These can be expected to have a strong effect on the simulated glacier mass balance. It is recommended to account for these shortcomings by applying correction procedures before using the RCM output for subsequent mass balance modeling. Despite the obvious model deficiencies in high-elevation regions, the new interface broadens the scope of application of glacier mass balance models and will allow for a straightforward assessment of future climate change impacts.

1. Introduction

During the past 100 years mountain regions all around the globe experienced considerable glacier mass losses and large reductions in glacier area (WGMS 2008). The European Alps, for instance, had lost about 50% of their 1850s ice mass by the 1980s (Haeberli and Hoelzle 1995) and melt rates even accelerated toward the end of the twentieth century (Paul et al. 2004; Zemp et al. 2008). Such variations in glacier mass are determined by the balance between incoming (mass gain) and outgoing (mass loss) terms and the underlying processes are strongly controlled by atmospheric factors.

To assess the response of a glacier's mass balance to changing atmospheric conditions, spatially distributed mass balance models (MBMs) were applied in numerous studies (e.g., Arnold et al. 1996; Hock 1999; Brock et al. 2000; Klok and Oerlemans 2002; Machguth et al. 2006). Depending on their complexity, these models incorporate a number of meteorological input parameters and simulate the temporal evolution of mass balance terms (accumulation and ablation) in the course of a year or over several years (Oerlemans 2001). The atmospheric forcing is usually provided by weather station data near to or on the glacier surface, which are interpolated to the required horizontal resolution of the

* Current affiliation: Institute for Atmospheric and Climate Science, ETH Zurich, Zurich, Switzerland.

Corresponding author address: Sven Kotlarski, Institute for Atmospheric and Climate Science, ETH Zurich, Universitaetstrasse 16, CH-8092 Zurich, Switzerland.
E-mail: sven.kotlarski@env.ethz.ch

DOI: 10.1175/2009JCLI2711.1

MBM. In most studies, only individual glaciers are considered (e.g., Stahl et al. 2008). The step to larger regions covering major river catchments or entire mountain ranges has only seldom been made, although distributed energy balance models are well suited for such large-scale applications. This can partly be explained by the fact that the application of an MBM to a large number of individual glaciers simultaneously requires both information on glacier characteristics [i.e., extent and a digital elevation model (DEM)] and atmospheric forcing datasets with a high spatial resolution for a large domain. In regions with good data coverage the latter can often be provided by interpolated station data. This is true for temperature and precipitation in the European Alps toward the end of the twentieth century. However, the data coverage is sparser in most other mountain regions, for other parameters than temperature and precipitation (e.g., global radiation) and for periods before the 1970s. For this reason, global applications like the assessment of the contribution of glacier melt to future sea level rise still apply a simplifying degree-day approach (e.g., Van de Wal and Wild 2001; Raper and Braithwaite 2006).

Instead of using interpolated station data as atmospheric forcing, an increasingly interesting option for the large-scale application of MBMs is to drive them with output of regional climate models (RCMs). In recent years, these models proved to be useful tools for the analysis of regional energy and water cycles as well as for the projection of climatic changes on a regional scale (e.g., Jacob et al. 2001; Kotlarski et al. 2005; Déqué et al. 2005; Jacob et al. 2007; Christensen and Christensen 2007). Similarly to general circulation models (GCMs), RCMs account for the most relevant processes, interactions and feedbacks between climate system components in a physically consistent manner, producing a comprehensive set of output data at a high horizontal resolution. In mountainous terrain the latter is important in order to resolve small-scale atmospheric circulations (e.g., those affected by orographic details of the land surface; Giorgi 1990; McGregor 1997). If driven by reanalysis or analysis data at the lateral boundaries (i.e., observation-based products describing the large-scale state of the atmosphere) RCMs are able to approximately reproduce observed spatial and temporal climatic patterns (e.g., Frei et al. 2003; Semmler and Jacob 2004; Kotlarski et al. 2005). Still, systematic errors and uncertainties of RCM data have to be considered for certain parameters (e.g., for precipitation in Alpine regions; Frei et al. 2003). Regarding the coupling to mass balance models a further point is the apparent scale gap. The currently available spatial resolution of multiyear RCM simulations (about 10–50 km) does not allow us to resolve individual glaciers and is much coarser than the resolution of state-of-the-art MBMs (10–100 m). This requires a further treatment of RCM results and the definition of an appropriate coupling interface between both models. Such an interface has to account for the further downscaling of RCM results to the target resolution of the MBM and could optionally also correct for systematic errors in the RCM output. Once this interface has been set up, the effects of regional climatic changes on glacier mass balance can be assessed in a straightforward way.

The present study, consisting of two separate parts, investigates the benefits and the limitations of forcing a distributed glacier mass balance model with the output of a state-of-the-art RCM. For this purpose, a test site in the south-central part of Switzerland was chosen that contains two glaciers of the Swiss mass balance network: Gries Glacier and Basòdino Glacier. For both glaciers a spatially distributed MBM is applied using 1) observational meteorological data from a nearby weather station (Robiei) and 2) the output of the regional climate model Regional Model (REMO). The first part of our study (this paper) presents and evaluates the RCM simulation that will be used to drive the MBM. A focus is laid on high-elevation regions and on those parameters that exert a primary influence on glacier mass balance and that will later on be used to drive the MBM (temperature, precipitation, global radiation). Specific questions that we are trying to answer are the following: to what extent can a state-of-the-art RCM reproduce the spatial and temporal variation of parameters relevant for glacier mass balance? Which biases do we have to expect in high-elevation regions and what is their seasonal and altitudinal variation? Is there a need for correcting RCM results before feeding them into a glacier mass balance model?

The second part of the study (Paul and Kotlarski 2010, hereafter Part II) describes the further downscaling of the RCM data to the resolution of the MBM and the results of the mass balance modeling, including the comparison of the simulated glacier mass balance to observations.

2. Data and methods

a. RCM data

Within the present study, the RCM REMO (Jacob and Podzun 1997; Jacob 2001; Jacob et al. 2001) was integrated for the period 1958–2002. REMO is a three-dimensional, hydrostatic atmospheric circulation model that is based on the numerical weather prediction model Europa-Modell (EM; Majewski 1991) and that includes the physical parameterization package of the general circulation model ECHAM4 (Roeckner et al. 1996). In the vertical, variations of the prognostic atmospheric

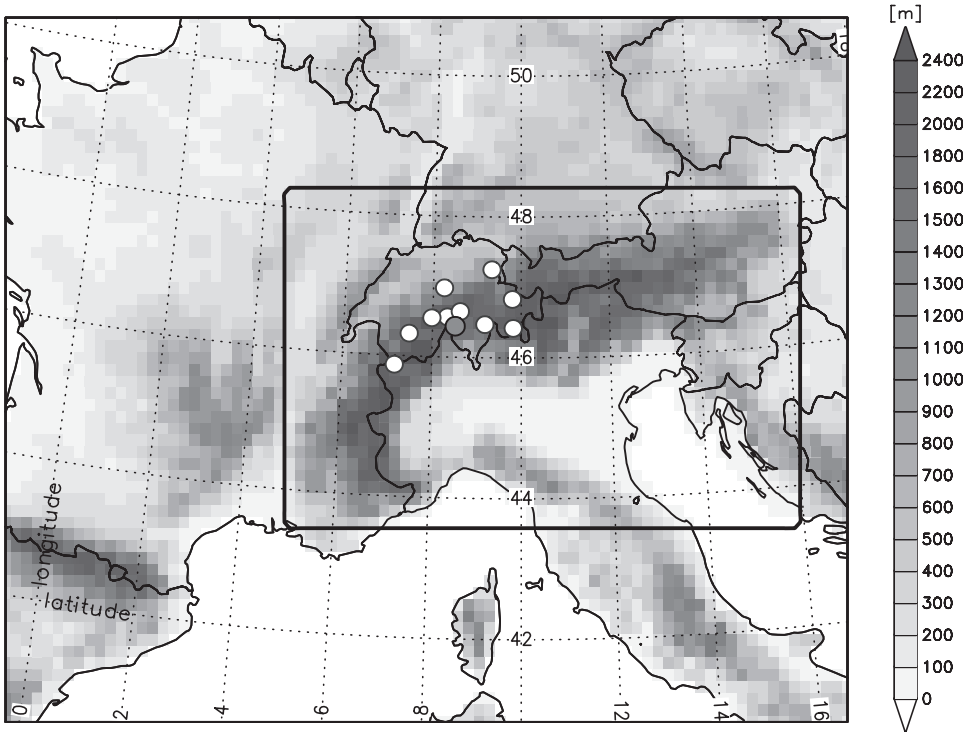

FIG. 1. REMO model domain and model orography (m). Each grid box corresponds to an area of approximately 18 km × 18 km. The black rectangle marks the Alpine subdomain in which the model validation is carried out. White circles show the location of the 10 MS measurement sites that are used for validation purposes. The gray circle corresponds to the location of the MS station Robiei close to Gries Glacier and Basòdino Glacier.

variables are represented by a hybrid vertical coordinate system (Simmons and Burridge 1981). For horizontal discretization REMO uses a rotated latitude–longitude coordinate system with standard grid spacings between 0.088° (approximately 10 km × 10 km) and 0.44° (approximately 50 km × 50 km). The lateral boundary conditions (LBCs) can either be provided by a GCM simulation or by reanalysis or analysis products. In all cases, the relaxation scheme according to Davies (1976) is applied: the prognostic variables of the RCM are adjusted toward the large-scale forcing in a lateral sponge zone of eight grid boxes with the LBC influence exponentially decreasing toward the inner model domain.

At the lower boundary REMO is forced by the land and sea surface characteristics (e.g., surface temperature, albedo, surface roughness length, etc.). The model version applied within this study (REMO 5.3) uses the so-called tile approach in which the total surface area of an individual model grid box can consist of a land, a water, and a sea ice fraction on a subgrid scale (expressed in percent). So far, glaciers are not explicitly represented in REMO's land surface scheme. In the European Alps their size is much smaller than the resolved scale of the RCM. Only the polar ice sheets are explicitly accounted for by a static, binary glacier mask that assigns ice surface characteristics to certain grid boxes and that does not change in time. The recent development of a glacier subgrid parameterization scheme that allows for a dynamic fractional ice coverage can be expected to improve this deficit (Kotlarski 2007).

For the present study, a model domain consisting of 81 × 61 grid boxes and completely covering the European Alps as well as further parts of central, western, and southern Europe was chosen (Fig. 1). The horizontal grid spacing is 1/6°, corresponding to a gridbox size of approximately 18 km × 18 km. In the vertical dimension 20 levels are used. The lateral boundary forcing for REMO is directly provided by the 40-yr European Centre for Medium-Range Weather Forecasts (ECMWF) Re-Analysis (ERA-40; for the period January 1958 to July 2002; Uppala et al. 2005) and the operational analysis of the ECMWF (for the remaining period August 2002 to December 2002). The internal model time step is 100 s.

In the chosen model setup the maximum value of the model topography (the mean elevation of the highest REMO grid box) is 2870 m. This value is only slightly larger than the steady-state equilibrium line altitude (i.e., the altitude of zero mass balance) in the Alps

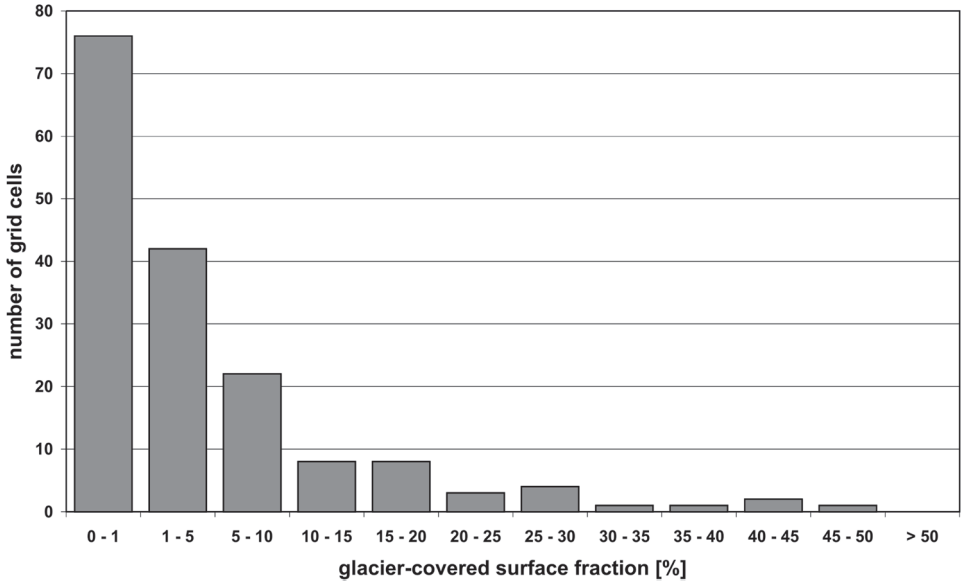

FIG. 2. Glacier-covered surface fraction of the REMO grid boxes based on the chosen model setup (1/6° horizontal resolution) and the Alpine-wide glacier inventory of the 1970s (WGMS 1989).

during the last decades of the twentieth century (>2700 m MSL in most regions; Zemp et al. 2007). This fact clearly illustrates that, if the model results are to be used in mass balance studies, a further downscaling of atmospheric parameters has to be carried out in order to provide a realistic atmospheric forcing at the site of individual glaciers. Based on the Alpine-wide glacier inventory of the 1970s (WGMS 1989), the maximum glacier-covered gridbox surface fraction in the current model setup is 46.7% (Jungfrau Region in central Switzerland). However, most glacierized grid boxes are only slightly glacierized with a glacier cover between 0% and 1% of the total surface fraction (Fig. 2). The relation between the area-weighted mean glacier altitude and the mean gridbox altitude (to which the RCM output parameters refer) is shown in Fig. 3 for the Swiss part of the model domain. In all grid boxes the mean glacier altitude is considerably higher than the mean gridbox altitude with deviations of more than 1000 m in regions with a low mean elevation. Assuming a temperature lapse rate of $-0.65°C\,(100\ m)^{-1}$, this altitude mismatch would lead to an overestimation of the near-surface air temperature by more than 6.5°C if the RCM output was directly used for driving the MBM. The difference between mean glacier altitude and gridbox altitude becomes smaller toward higher elevations (slope of regression line smaller than 1 in Fig. 3).

b. Observational data

Several observation-based datasets are used as a reference for evaluating the RCM's performance. For air temperature, the model validation is based on the gridded monthly climatology of the Climatic Research Unit (CRU) TS 1.2 dataset (Mitchell et al. 2004; subperiod used: 1958–2000). Additionally, the modeled air temperature is compared against the mean monthly temperature climatology of 10 high-elevation stations of the Swiss automatic network (ANETZ; period: 1961–90; see Fig. 1 for station locations). This dataset was provided by MeteoSwiss (MS), the Swiss Federal Office of Meteorology and Climatology.

The CRU TS 1.2 dataset is also used as reference for simulated precipitation, in addition to the Alpine-wide ALP-IMP/HISTALP precipitation dataset (Efthymiadis et al. 2006; subperiod used: 1958–2000). Both are provided on a regular 1/6° grid (i.e., in a similar horizontal resolution as used by REMO) and do not account for the systematic bias of rain gauge measurements, the most significant of which is undercatch of solid precipitation (snowfall; New et al. 2000). For the period 1971–1990 the ALP-IMP/HISTALP dataset makes use of the very high-resolution Alpine precipitation climatology of Schwarb (2000). In the second part of the present study (Part II), the latter is used for a local scaling of RCM-simulated precipitation.

As observation-based gridded datasets are not available for global radiation, the validation of this parameter solely relies on quality-checked observational data for individual stations. For this purpose, the mean annual cycle of global radiation was derived for 10 high-elevation measurement sites in the Alpine region (Fig. 1) based on the MeteoSwiss (MS) automatic observational network

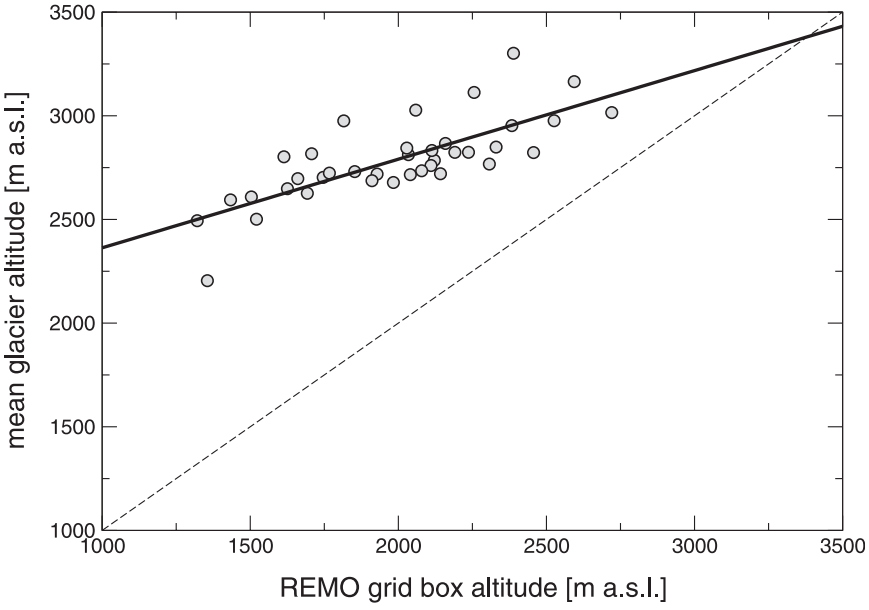

FIG. 3. Relation between the REMO gridbox altitude (x axis) and the area-weighted mean glacier altitude (y axis) for the Swiss part of the model domain. Glacier altitude and area are based on the Alpine-wide glacier inventory of the 1970s (WGMS 1989). Each dot represents one glacierized REMO grid box. The dashed line denotes the 1:1 relation and the bold black line shows the best linear fit as obtained by linear regression ($r = 0.76$).

(ANETZ; period: 1981–2000). With one exception (Ulrichen instead of Grimsel) these stations are the same as used for validating the RCM-simulated 2-m temperature (see above).

In addition to model validation on an Alpine-wide scale, with a focus on high-elevation regions, a special analysis is carried out for the observation site of Robiei. This ANETZ station of MeteoSwiss is located at an altitude of 1898 m in southern Switzerland (see Fig. 1), close to Gries and Basòdino Glacier. The mass balance modeling for these two glaciers will use both REMO data and Robiei station data as input. It is thus of high importance to assess the general performance of REMO in this region with respect to all forcing parameters of the MBM. Observational data for the Robiei station were available for a period of 10 yr (1991–2000). In the case of temperature, the respective CRU TS 1.2 grid box is also analyzed for this period.

c. Evaluation methods

As the Alps are our focus region, the RCM evaluation is carried out for the Alpine part of the model domain only (see Fig. 1, land grid boxes only). Given the temporal resolution of most observational datasets used, the evaluation is generally based on monthly values (monthly means and sums). In the case of the gridded CRU and ALP-IMP datasets, observations and model results are compared to each other for distinct elevation intervals and on a gridbox basis. For this purpose, the CRU and ALP-IMP datasets were conservatively remapped to the rotated 1/6° RCM grid. To account for the pronounced height dependence of near-surface air temperature, elevation differences between the observational grid and the RCM grid are accounted for by additionally applying a temperature lapse rate (see below). In general, the effect of the remapping on the spatial patterns of temperature and precipitation is small since both the observational data and the RCM data are provided on a 1/6° grid, which is regular in case of the observations and rotated in case of the RCM. Gridbox areas are similar in both cases. For model validation based on distinct elevation intervals, the grid boxes within the Alpine part of the model domain were pooled into the three elevation classes <1000, 1000–2000, and >2000 m. These classes represent 77%, 18%, and 5% of the entire Alpine model domain, respectively.

For the station-based validation of 2-m temperature and global radiation, the observed annual cycles at individual measurement sites are compared against the simulated values for the model grid box in which the respective station is located. A smoothing of the RCM-simulated spatial patterns, which can be useful especially for precipitation in order to account for numerical uncertainty on a gridpoint scale, is not carried out because the variability at the RCM grid scale could be

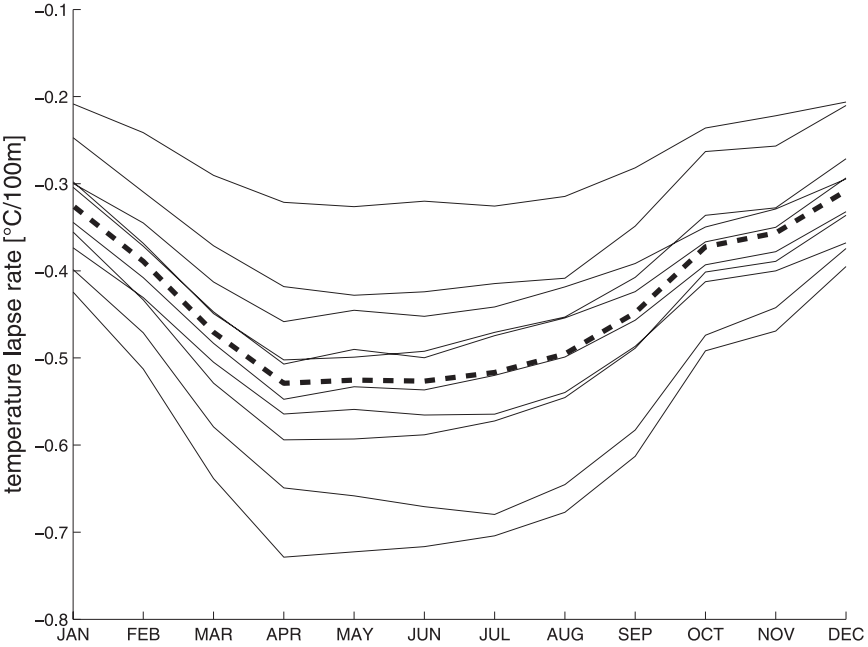

FIG. 4. Annual cycle of temperature lapse rates for 10 different regions in the Alps (thin lines) based on the CRU TS 1.2 dataset (period 1961–90). Each region corresponds to 5 × 5 CRU grid boxes with a MeteoSwiss station located in the center grid box. The arithmetic mean of the 10 regional lapse rates is indicated by the thick dashed line.

important for mass balance forcing. Furthermore, the use of nonsmoothed fields allows for a better visibility of shortcomings of the native RCM dataset. In the case of 2-m temperature, the elevation difference between the RCM grid box and the measurement site is explicitly accounted for by applying a monthly and regionally varying temperature lapse rate to the model output. For this purpose, monthly lapse rates for the period 1961–90 were computed for the surroundings of each individual MeteoSwiss measurement site based on the CRU TS 1.2 temperature dataset (see above). Lapse rates were derived by regressing the mean monthly temperature at 25 CRU grid boxes (square of 5 × 5 boxes with the measurement site located in the center grid box) against the respective CRU gridbox elevation. Figure 4 shows the obtained annual cycles of the temperature lapse rate (i.e., of the regression coefficients) for each of the 10 regions as well as the mean monthly lapse rate averaged over all regions. In all cases the temperature decrease with altitude exhibits a distinct annual cycle with small decreases in wintertime [lapse rates mostly between −0.4° and −0.2°C (100 m)$^{-1}$] and largest decreases during the summer months [lapse rates up to −0.73°C (100 m)$^{-1}$]. The smaller mean values in winter can be explained by a more stable layering and a higher inversion frequency. Pronounced differences exist between the individual regions, but in most cases lapse rates are well below the often assumed standard value of −0.65°C (100 m)$^{-1}$. Applying a constant lapse rate of −0.65°C (100 m)$^{-1}$ could therefore lead to important errors in the analysis if the elevation difference between a measurement site and the respective RCM grid box is large. This is especially true for the winter months when the CRU-based lapse rates are small. To obtain some idea on the difference between the two observation-based datasets (MS and CRU), the gridded CRU temperatures are also compared to the individual station time series. Here, the same height-correction procedure is applied.

3. Results

a. Temperature

As can be seen from Fig. 5, the general temporal evolution of the simulated mean Alpine 2-m temperature is in very good agreement with the CRU dataset (top-left panel). The interannual variability, expressed by the standard deviation of both time series, is well represented and both the comparatively cold period between the 1970s and the early 1980s and the rising temperatures toward the end of the century are captured by the model. However, in most years the observed mean temperature is underestimated by REMO with largest differences of up to 1°C in the 1970s and the late

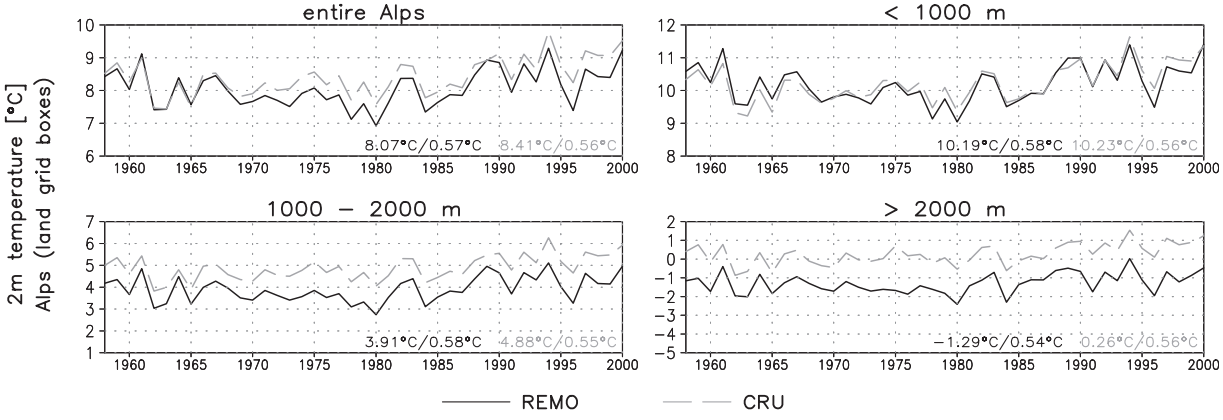

FIG. 5. Comparison of the simulated (REMO) and the observed (CRU) 2-m temperature for the period 1958–2000 (annual means) in the entire Alpine region and for three distinct elevation bands. The numbers in the lower-right corner of each panel represent the mean value/standard deviation of the individual time series (no detrending carried out).

1990s. The mean temperature bias of REMO over the entire period amounts to −0.34°C (cf. 8.07°C and 8.41°C). This cold bias is caused by a clear underestimation of temperature in grid boxes above 1000 m (Fig. 5, bottom panels), that is, in those regions where most glaciers in the Alps are located. The temperature bias in the 1000–2000- and >2000-m elevation intervals amounts to −0.97° and −1.55°C, respectively. In individual years, the observed temperature is underestimated by more than 2°C in high-elevation regions above 2000 m. This strong bias of mean annual temperature at high elevations can primarily be attributed to the winter months, when the simulated 2-m temperature shows a cold bias of about −2°C for the elevation interval 1000–2000 m and an even larger bias up to −4°C in grid boxes above 2000 m (Fig. 6, bottom panels). In regions below 1000 m, which represent more than 75% of the Alpine region investigated here, the mean annual cycle of temperature is very well reproduced (bias between −0.4° and 0.4°C in any month; top-right panel in Fig. 6).

In principle, the apparent cold temperature bias in high-elevation regions with respect to the CRU dataset could be due to an inappropriate treatment of the governing processes in the RCM. It could also be caused by a systematic temperature bias in the gridded observational dataset itself due to an underrepresentation of high elevation sites and an inappropriate spatial (both horizontal and vertical) interpolation procedure. To rule out the latter possibility, an additional validation of the simulated 2-m temperature is carried out using the data of 10 individual stations of the MS observational network (see above). Figure 7 shows the comparison between the mean annual cycle of temperature for the period 1961–90 at these sites (MS), the simulated temperature for the respective REMO grid box and the observation-based temperature of the respective CRU grid box. To account for the elevation difference between an individual MS station and the REMO/CRU gridbox altitude, the REMO/CRU data are height corrected (see section 2c). In general, the results obtained

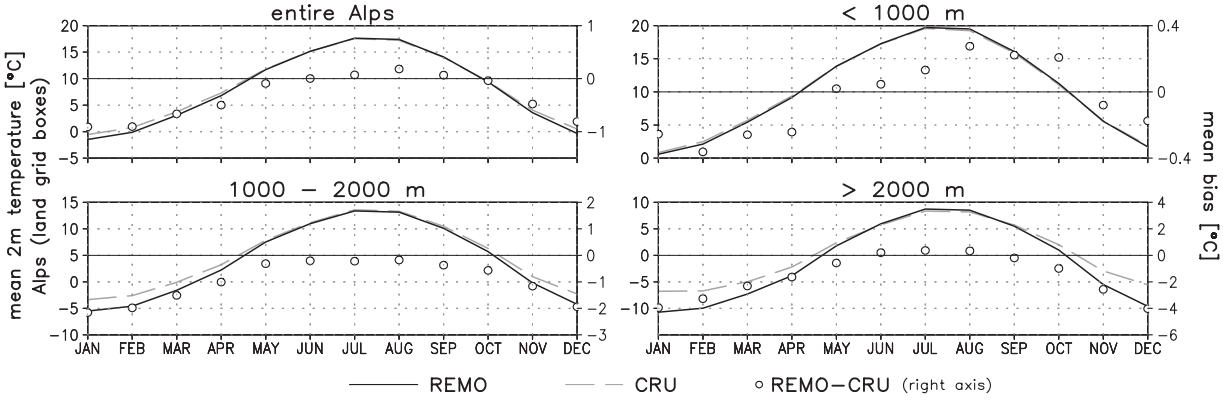

FIG. 6. Comparison of the simulated (REMO) and the observed (CRU) mean annual cycle of 2-m temperature (1958–2000) in the entire Alpine region and for three distinct elevation bands. The circles represent the mean monthly temperature bias (right axis).

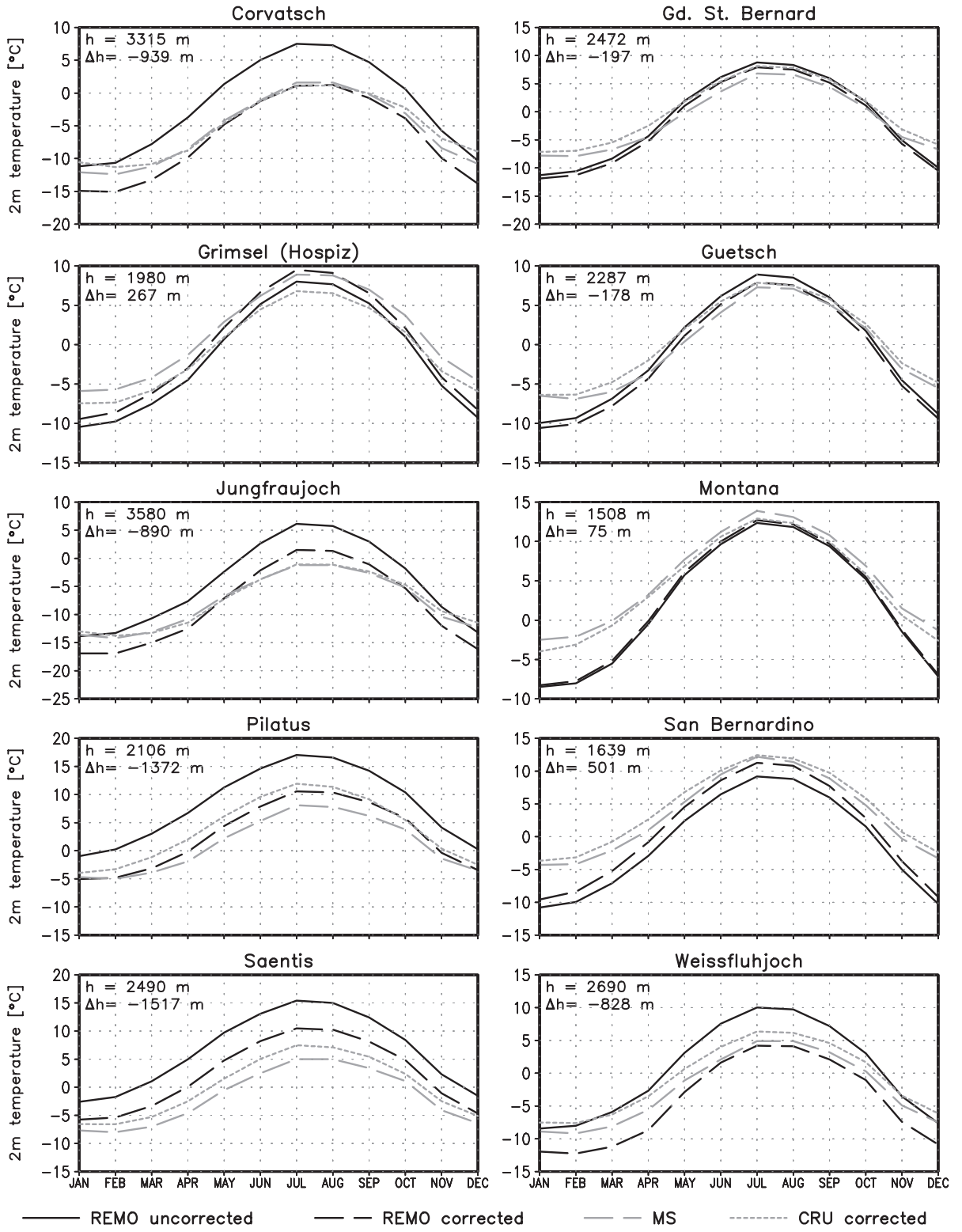

FIG. 7. Comparison of the simulated (REMO) and the observed (MS, CRU) mean annual cycle of 2-m temperature (1961–90) at 10 high-elevation observation sites. The REMO/CRU annual cycles refer to the model grid box in which the observation site (MS) is located. REMO data are shown with and without correction for the elevation difference between REMO grid box and observation site (see text). Similarly, the grid-based CRU data are height corrected to match the MS observation site altitude. h: Elevation of the measurement site. Δh: Elevation difference REMO grid box–measurement site.

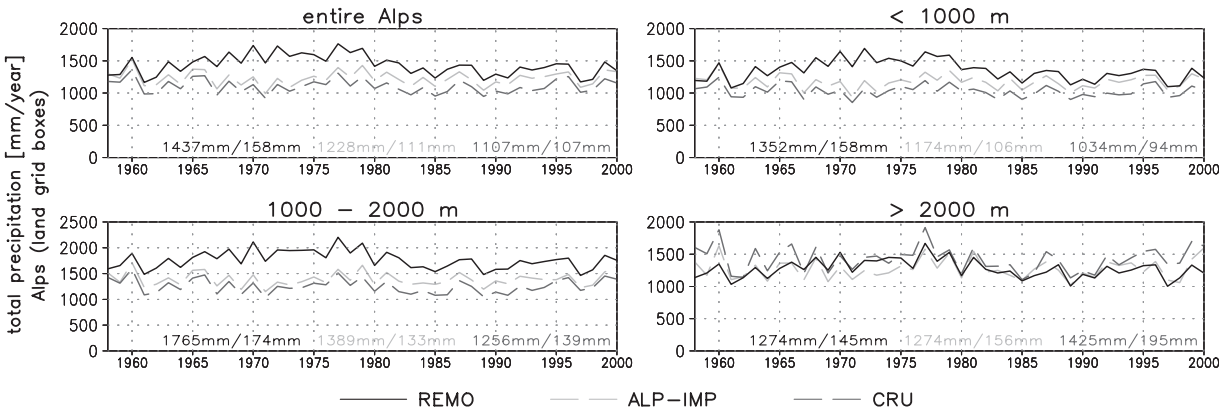

FIG. 8. Comparison of simulated (REMO) and observed (ALP-IMP, CRU) precipitation for the period 1958–2000 (annual sums) in the entire Alpine region and for three distinct elevation bands. The numbers in the lower part of each panel represent the mean value/standard deviation of the individual time series (no detrending carried out).

for the individual elevation intervals are confirmed in this analysis. Except for Pilatus and Saentis, the height-corrected REMO temperature shows a pronounced cold bias with respect to the MS observations in winter. This is true for stations that lie above the mean REMO gridbox altitude (e.g., Corvatsch, Jungfraujoch, and Weissfluhjoch) and for stations with a lower elevation (e.g., Grimsel and San Bernardino). Hence, the obvious underestimation of wintertime temperature is probably not due to wrong assumptions concerning the temperature lapse rate in this season (which is applied during the height-correction procedure) but rather points to a systematic model bias. In summer, on the other hand, the simulated height-corrected temperature is relatively close to the MS observations. The only exceptions are Jungfraujoch, Pilatus, and Saentis, where REMO shows a positive summer bias of more than 2°C. At these sites the measurement station is located at a much higher altitude than the respective REMO grid box and the model bias could partly be caused by inaccuracies in the height-correction procedure (i.e., by errors in the temperature lapse rate assumed for the summer months).

At most sites, the height-corrected temperature of the CRU dataset approximately corresponds to the MS data. Exceptions are Grimsel and Pilatus where CRU and MS disagree by more than 2°C during the summer months. Generally, the pronounced negative wintertime bias of REMO with respect to the MS observations is larger than the difference between the two observational datasets, which points to a ''true'' and systematic model bias rather than to inaccuracies in the reference datasets.

b. Precipitation

The comparison of the temporal evolution of the simulated and observed annual precipitation sums for the entire Alps (Fig. 8, top-left panel) reveals a systematic wet bias of REMO that is strongest in the late 1960s and the 1970s. Over the entire investigated period REMO overestimates mean annual precipitation by 17% with respect to ALP-IMP (cf. 1437 and 1228 mm yr^{-1}) and by almost 30% with respect to CRU (cf. 1437 and 1107 mm yr^{-1}). In individual years during the 1970s, precipitation is overestimated by up to 40%. This apparent wet bias would be less pronounced if the observational datasets were corrected for the systematic undercatch of precipitation, which can be more than 50% in the case of snowfall (e.g., Sevruk 1982; Forland and Aune 1985). In contrast, the interannual variability of the observed precipitation sums is well captured by the model. Concerning the representation of ''reality'' by the two observational datasets, it should be noted that CRU and ALP-IMP differ from each other, especially toward the end of the twentieth century (higher amounts of precipitation in ALP-IMP). In this period, the difference between ALP-IMP and CRU is larger than the difference between REMO and ALP-IMP.

With respect to discrete elevation belts (Fig. 8, top-right and bottom panels) it becomes evident that the wet precipitation bias is caused by an overestimation in regions below 2000 m, which cover about 95% of the total area under investigation and, hence, dominate the Alpine mean value. With respect to ALP-IMP (CRU) annual precipitation is overestimated by 15% (31%) in regions below 1000 m and by 27% (41%) at elevations between 1000 and 2000 m. In grid boxes above 2000-m observed precipitation is either slightly underestimated by the model (bias of −11% against CRU) or very well captured (exact match against ALP-IMP). However, a correction of the observation-based values for the systematic rain gauge undercatch (see above) would result in a clear dry bias also with respect to ALP-IMP.

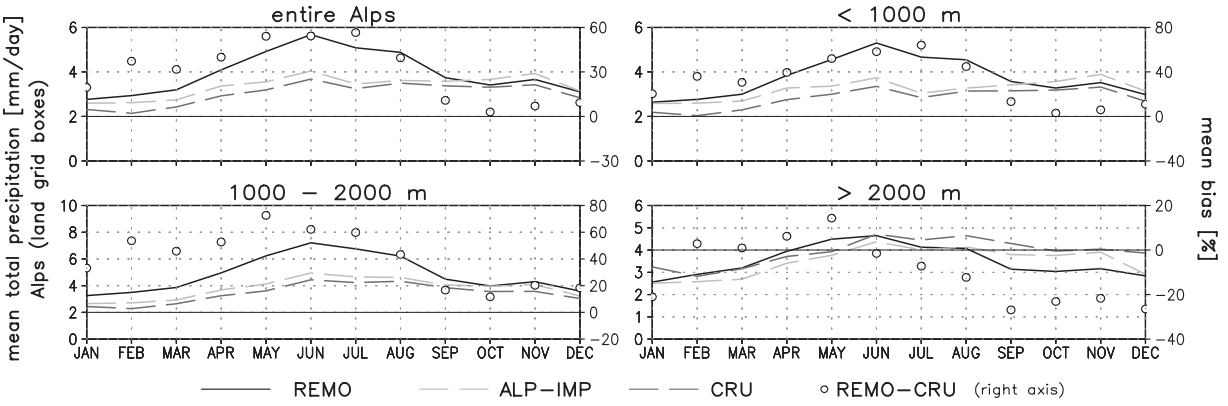

FIG. 9. Comparison of the simulated (REMO) and the observed (ALP-IMP, CRU) mean annual cycle of precipitation (1958–2000) in the entire Alpine region and for three distinct elevation bands. The circles represent the mean monthly precipitation bias (right axis).

The negative precipitation bias of REMO at high altitudes (>2000 m) primarily stems from an underestimation in autumn and winter. In these months the negative bias lies between −20% and −30% with respect to CRU (Fig. 9, bottom-right panel). At elevations below 2000 m the general wet bias is mainly due to an overestimation of precipitation in spring and summer (Fig. 9, top-right and bottom-left panels). In individual months the positive bias with respect to CRU can amount to more than 60%. The obvious dependency of the precipitation bias on both gridbox altitude and season can also be derived from Fig. 10, which shows the seasonal

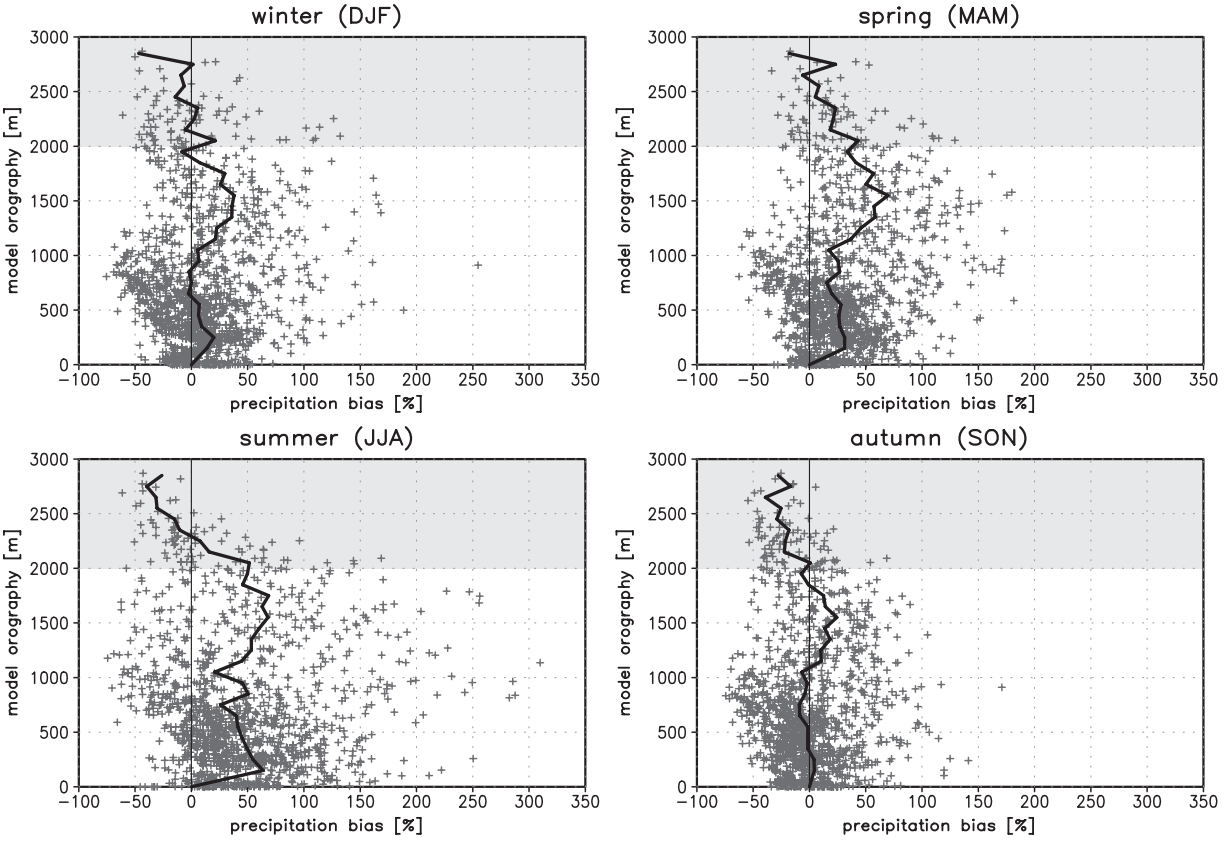

FIG. 10. Seasonal precipitation bias [REMO–ALP-IMP (%)] vs model orography for the Alpine subdomain (see Fig. 1). Each marker represents one REMO grid box. Grid boxes with an orography >2000 m are found in the gray-shaded area. The black line represents the mean precipitation bias based on 100-m elevation intervals (0–99, 100–199, . . .; arithmetic means of individual gridbox biases).

precipitation bias for each individual grid box against altitude. The black line in each panel denotes the mean bias for each 100-m elevation interval (arithmetic mean of individual gridbox biases). In addition to the general dependence of the precipitation bias on the altitude, Fig. 10 also reveals that elevation is not the only controlling factor. The seasonal bias is subject to a considerable spread between individual grid boxes of the same elevation interval. In summertime, for instance, precipitation biases in grid boxes above 2000-m range from −60% to +170% (bottom-left panel). Still, the majority of high-elevation boxes shows a clear underestimation of precipitation in summer, autumn, and winter, which is in some cases larger than 50% (top-left and bottom panels). With increasing elevation the negative bias generally becomes more pronounced. In individual high-elevation grid boxes, precipitation can also be overestimated by more than 50%. In contrast to this, springtime precipitation is overestimated by the model in most grid boxes independent of their altitude (top-right panel). In all seasons the maximum mean precipitation bias is found at altitudes between 1500 and 1800 m. The largest positive biases arise in the summer season and below 2000 m, with an overestimation of precipitation by more than 250% in individual grid boxes (bottom-left panel).

The strong overestimation of summertime precipitation in large parts of the study region also becomes evident when comparing the simulated and the observed (ALP-IMP) spatial patterns of mean seasonal precipitation (Fig. 11). A large number of grid boxes in the Alpine region show a clear positive bias of more than 60% in summer. Still, precipitation in regions along the southern Alpine ridge (southern Switzerland) and along the ridge of the Jura Mountains (northwestern border of Switzerland) is considerably underestimated by the model. This discrepancy between the precipitation bias at grid boxes located along local orographic maxima (negative bias) and their neighboring regions (strong positive bias) becomes even more evident in winter (top panels in Fig. 11). Apparently, the model systematically dislocates precipitation from ridges to the forelands causing a negative precipitation bias at high-elevation sites in all seasons. The large-scale seasonal precipitation patterns (highest precipitation sums in the Alpine region except for some dry inner-alpine regions, lower sums in the surrounding regions) are still well captured by the model.

c. Global radiation

Global radiation often constitutes the primary source of melt energy on glaciers and plays a key role for glacier mass balance (e.g., Oerlemans 2001). An accurate description of the global radiation flux is therefore of high importance in mass balance modeling. In the RCM downscaling approach presented in Part II, the global radiation flux as simulated by REMO is used as an input for the distributed MBM.

Figure 12 presents a comparison between the simulated (REMO) and the observed (MS) mean annual cycle of global radiation for 10 high-elevation measurement sites of the Swiss automatic network, all of them located above 1300 m. Model and observations are in good agreement with respect to the basic characteristics of the annual cycle (mean value and amplitude). Still, important and systematic model biases arise in individual seasons. At all sites the mean monthly radiation bias (circles in Fig. 12) is subject to a pronounced variability on a monthly basis with maximum values in summer (July or August, depending on the site, but positive in all cases) and a minimum in spring (March or April, depending on the site as well, but negative in all cases). At most stations the positive radiation bias in summer amounts to several tens of watts per meters squared with maximum values up to 60 W m^{-2} (July at Pilatus). In contrast to this, a systematic negative bias of the simulated global radiation flux seems to prevail in winter and especially in spring. Here, observations are underestimated by more than 50 W m^{-2} at individual stations (Corvatsch, Guetsch, Jungfraujoch, and Weissfluhjoch). The only exception is the valley station of Ulrichen where the simulated springtime global radiation flux corresponds very well to the observations and negative biases are smaller than 20 W m^{-2}. At very high altitudes (Corvatsch, Gd. St. Bernard, Jungfraujoch, Saentis, and Weissfluhjoch), the combination of a negative radiation bias in spring and a positive summer bias results in a backward shift of the annual maximum of global radiation by 1–2 months from April–May to June–July in the model simulation compared to observations.

d. Focus Robiei

In addition to the Alpine-wide analysis presented above, the performance of REMO is assessed in detail for the site of Robiei. This station is located close to Gries and Basòdino Glacier, the two glaciers under investigation in Part II of this study. Figure 13 shows a comparison of the simulated annual cycle for temperature, precipitation, and global radiation against Robiei station data (and against CRU in case of temperature) for the period 1991–2000. This analysis basically confirms the results of the Alpine-wide model evaluation: systematic model biases that were discovered on the Alpine scale are also found for the specific site of Robiei. For instance, REMO strongly underestimates wintertime temperature with respect to the Robiei station data and the respective CRU grid box (left panel). Biases are

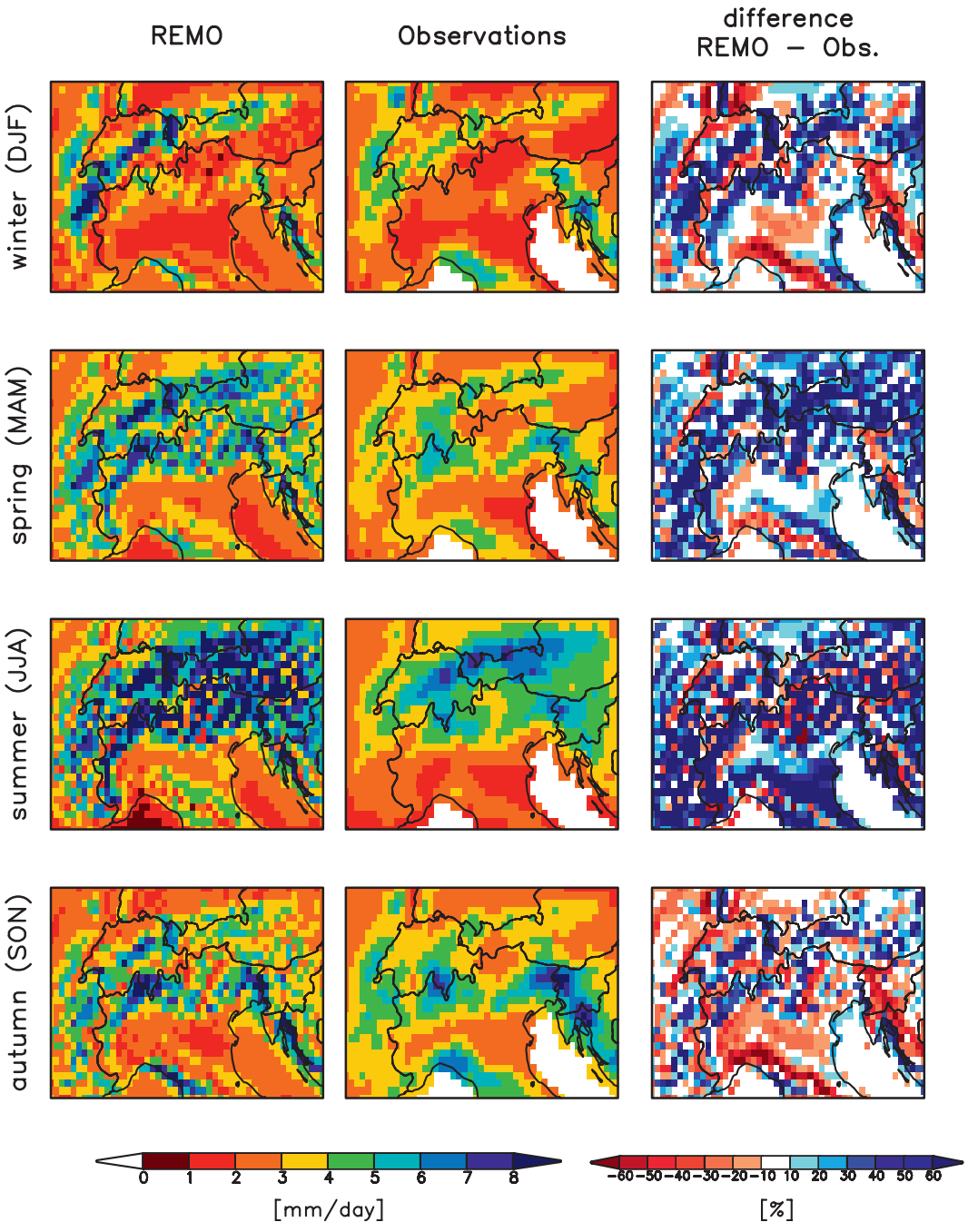

FIG. 11. Comparison of simulated and observed mean seasonal precipitation patterns in the Alpine region for the period 1958–2000: (left) REMO (mm day^{-1}), (middle) ALP-IMP (mm day^{-1}), and (right) difference between REMO and ALP-IMP (%).

largest in December and January with an underestimation of temperature by more than 4°C. In summer, a small negative bias is still present but is far less pronounced (underestimation by less than 2°C in all months). Only in the case of precipitation (middle panel) does the model validation for Robiei reveal different bias characteristics compared to the Alpine-wide analysis. Because of an underestimation of precipitation in most months with negative biases of up to −66% in January and February, the annual precipitation sum is underestimated by about one-third (cf. 1722 and 2550 mm yr^{-1}). The most striking discrepancy between model and

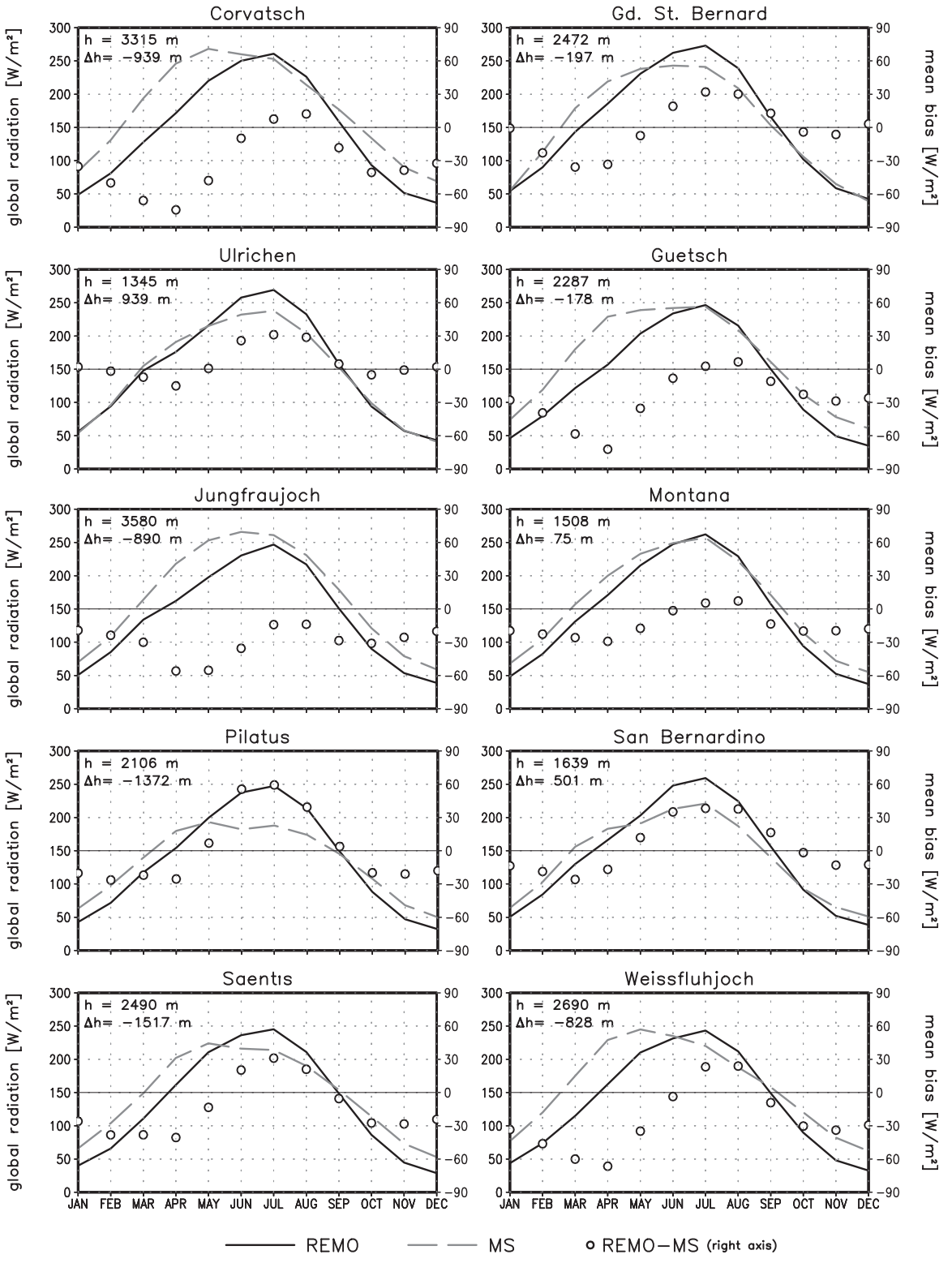

FIG. 12. Comparison of the simulated (REMO) and the observed (MS) mean annual cycle of global radiation (1981–2000) at 10 high-elevation observation sites. The simulated annual cycles refer to the model grid box in which the observation site is located. The circles represent the mean monthly radiation bias (right axis). h: Elevation of the measurement site. Δh: Elevation difference REMO grid box–measurement site.

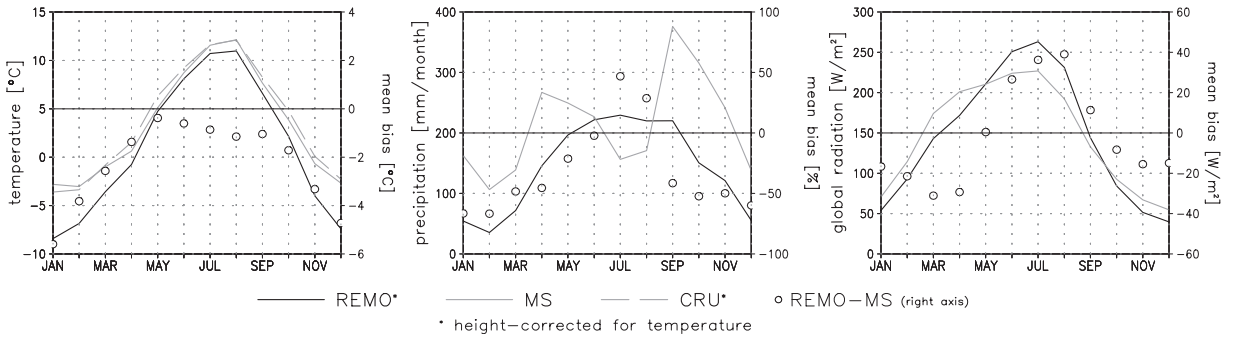

FIG. 13. Comparison of the simulated (REMO) and observed (MS, CRU) annual cycles of (left) temperature, (middle) precipitation, and (right) global radiation for the site of Robiei and the period 1991–2000. REMO and CRU temperature data are height corrected in order to account for the elevation difference between the REMO grid box and the Robiei observation site (see text). The circles represent the mean monthly bias of REMO with respect to MS (right axis).

observations is the absence of the secondary summertime precipitation minimum in the simulated annual cycle. This minimum, which is presumably related to the specific setting of the observation site within the regional topographic context, is not captured by REMO, leading to an overestimation of precipitation by 47% and 29% in July and August, respectively. For global radiation the results of the Alpine-wide analysis are again confirmed (right panel). While the simulated radiation fluxes are too low in winter and spring (negative biases up to 31 W m^{-2} in March), REMO clearly overestimates global radiation in summer with positive biases up to 39 W m^{-2} in August.

4. Discussion

The validation presented above reveals that the spatiotemporal variability of the climatic parameters used to drive a glacier mass balance model at a later stage (temperature, precipitation, global radiation) is basically reproduced by the RCM REMO. Compared to the CRU dataset the Alpine mean temperature is underestimated by 0.34°C. Annual precipitation shows a positive bias of 17% (30%) with respect to the uncorrected gridded ALPIMP (CRU) dataset. Still, a number of major shortcomings appear, especially in high-elevation regions. In this respect, one of the most important parameters is wintertime precipitation, which is responsible for the majority of snow accumulation on Alpine glaciers. The validation of the simulated precipitation sums in winter indicates a clear overestimation in grid boxes between 1000 and 2000 m during the 1970s and 1980s. Feeding these values directly into the MBM (i.e., without a further correction of the model bias) would result in an overestimation of snow accumulation and, consequently, of glacier mass balance. The situation is different in high-elevation regions above 2000 m. Here, simulated wintertime precipitation is slightly underestimated in most grid boxes, potentially causing a negative effect on glacier mass balance. This underestimation of winter precipitation is also true for the case of the Robiei measurement site, which is located in the vicinity of the two glaciers under consideration in Part II of this study. However, at this specific site the precipitation bias is much more pronounced than on an Alpine-wide scale. The bimodal annual cycle of observed precipitation is not captured by REMO and wintertime precipitation is underestimated by more than 60%. Robiei therefore has to be considered as an extreme case in which the forcing of a glacier mass balance model without correcting for the strong precipitation bias does not seem meaningful. The situation might be different at other sites where observed and simulated amounts of wintertime precipitation are in better agreement.

A detailed analysis of the causes of the obvious systematic model bias in the spatial precipitation pattern (underestimation at high-elevation ridges, overestimation at lower elevations) is beyond the scope of this study. Very probably, the bias is partly connected to the horizontal advection of falling hydrometeors by wind. Assuming a range of possible terminal fall speeds for rain droplets and snowflakes and of plausible horizontal wind speeds (5–30 m s^{-1}), a particle originating at an altitude of 3000 m can get advected between 1.5 and 90 km before reaching the ground (Roe 2005). In the most extreme case and with a horizontal RCM resolution of 18 km this would mean a displacement of precipitation by up to 5 grid boxes in the downwind direction. Despite the potential effect of this process on the simulated precipitation pattern, the horizontal advection of hydrometeors is not accounted for in the REMO version applied here: orographic lifting of advected air masses causes condensation and the generation of rain- and/or snowfall, which reaches the ground

in the same time step at the base of the vertical gridbox column. This neglect of the advection of falling precipitation can lead to a systematic overestimation of precipitation on the windward slopes and an underestimation downwind. The recent development of an online advection scheme for precipitation (Göttel 2009) shows that the explicit consideration of the drift of falling hydrometeors can considerably reduce the precipitation bias of REMO at high altitudes. Göttel (2009) applied REMO at a horizontal resolution of about 10 km $\times$ 10 km, but it can be expected that a similar effect, though less pronounced, would appear for the resolution applied in the present study (18 km $\times$ 18 km).

A further reason for the elevation-dependent precipitation bias could be the use of a nonsmoothed model topography, which can lead to sharp gradients of topography between adjacent grid boxes and the generation of small-scale gravity waves. On the coarse model grid scale, the latter can only be represented in an approximate manner which potentially causes a dislocation of zones of up- and downdraft (e.g., Gaßmann 2002). This, in turn, could result in a too early condensation of atmospheric water vapor and a too early occurrence of rain- and snowfall when humid air masses are lifted by an orographic obstacle.

Besides the model's precipitation bias a further important point for mass balance modeling is the cold temperature bias at high altitudes for most parts of the year. This bias would generally lead to an overestimation of the fraction of solid precipitation (snowfall) and, hence, to an increase in snow accumulation with a positive effect on glacier mass balance. The general underestimation of temperature would also cause a reduction of melt rates through a reduced flux of sensible heat toward the glacier surface, resulting in a positive bias of glacier mass balance. However, summer temperature biases (which are less pronounced in REMO) are much more important for this effect than inaccuracies in modeled winter temperature (which is strongly underestimated by REMO). A positive effect on glacier mass balance can also be assumed for the negative bias of springtime global radiation at high-elevation sites. This phenomenon can possibly be attributed to errors in the simulated cloud cover since clouds exert a primary influence on the incoming surface radiation fluxes. A possible overestimation of springtime cloud cover could be connected to the overestimation of precipitation in most grid boxes in this season (see above), indicating that a general positive bias of large-scale humidity might be a further possible reason for the precipitation bias of REMO.

Model deficiencies related to clouds and their influence on radiative processes are probably also responsible for the systematic overestimation of global radiation at high-elevation sites in summer. Here, the lower radiation flux in the observational dataset might be connected to orographically induced convective activity and the formation of convective clouds. These processes are not explicitly resolved by the RCM. They are treated by the model's convection parameterization scheme in a strongly simplified manner and without a direct influence of convective clouds on radiative processes. Concerning the larger observed solar radiation flux in winter and spring, a further reason could be multiple reflection of solar radiation on surrounding snow-covered slopes, a process that is also not considered in REMO.

Finally, it should be mentioned that in the region of interest (in high-altitude Alpine terrain) the coverage of meteorological stations is usually very sparse and errors of meteorological measurements themselves are largest. The uncertainty of observation-based datasets used for model validation is thus relatively large, especially in the case of precipitation.

5. Conclusions

The present study investigates the potential of using RCM output as an atmospheric forcing for distributed glacier mass balance models in the European Alps, a region with a complex topography and a high spatial variability of atmospheric quantities. The detailed validation of those parameters that will serve as input to the mass balance model (near-surface air temperature, precipitation, and global radiation) shows that the basic spatial and temporal variabilities of all three parameters are reproduced by REMO. This provides confidence in the general applicability of REMO data for mass balance modeling. However, regarding the specific questions raised in the introductory chapter, important and systematic RCM deficiencies are detected at high elevations. If applied without further bias correction, some of these deficiencies have a high potential to cause errors in the subsequent simulation of glacier mass balance [viz., the bias of winter precipitation (positive or negative, depending primarily on gridbox altitude), the negative temperature bias in winter, and the overestimation of summertime global radiation]. It is thus recommended to account for these known deficiencies by applying correction procedures before using the RCM output for subsequent impact studies. Implicitly, such a correction could also account for inconsistencies in the atmospheric forcing related to different surface conditions in the RCM and the MBM, respectively (e.g., ice-free surface in the RCM versus ice-covered surface in the MBM). Concerning climate change studies, the general question arises whether RCM biases are stationary in time

(i.e., whether the same correction can be applied for today's and for future climatic conditions). There is strong evidence that this assumption is not necessarily valid (Christensen et al. 2008). We also fully recognize that different RCMs might perform differently in high-mountain topography. These aspects have been and are still under investigation in several model intercomparison studies such as the Prediction of Regional Scenarios and Uncertainties for Defining European Climate Change Risks and Effects (PRUDENCE; Christensen et al. 2007) and Ensemble-based Predictions of Climate Changes and their Impacts (ENSEMBLES) (Hewitt 2005). We start here with just one single RCM in order to investigate the principal challenges of an RCM–MBM coupling.

Whether RCM biases are corrected prior to forcing an MBM or not, a further downscaling of the RCM output to the scale required by distributed MBMs is necessary. Although the RCM resolution used in the present study (approximately 18 km $\times$ 18 km) is comparatively high, it does not yet correspond to the MBM scale. The same is true for most other impact models (e.g., catchment-scale water balance models). A straightforward way to bridge the apparent scale gap is the further redistribution of atmospheric quantities on the RCM subgrid scale using high-resolution observational datasets (local scaling of precipitation) and/or a known altitudinal dependence of parameters like precipitation and temperature. Local scaling of RCM-simulated precipitation could also be combined with a bias correction as applied in Widmann et al. (2003) and Früh et al. (2006). For the present two-part study we have decided to first present the original RCM output in Part I (in order to detect principle RCM shortcomings) and to bridge the scale gap for the specific application of the impact model afterward (Part II).

Despite the encountered RCM biases at high elevations, a number of obvious advantages justify the use of RCM data as an input to glacier mass balance models. Especially in regions with a low density of meteorological measurement networks, RCMs can provide useful information on the scale of entire mountain ranges. This, however, implies that systematic model biases are known and could be corrected for. Furthermore, the development of an RCM–MBM interface will facilitate the use of RCM climate change scenarios for the assessment of future changes in glacier area and volume. One advantage of this physical downscaling method compared to a statistical downscaling of coarse-resolution GCM climate change signals to the sites of individual glaciers (e.g., Schneeberger et al. 2001; Reichert et al. 2002; Radić and Hock 2006) is that an RCM responds in a physically consistent way to different external forcings, such as changes in atmospheric greenhouse gas concentrations (Wilby et al. 2000). Unless the RCM output is being postprocessed on an individual-parameter basis (e.g., bias correction for individual output parameters) the relation between the simulated values of, for example, precipitation, air temperature, and radiation is physically consistent and meaningful. The full potential of such an approach could only be exploited with an MBM that is based on the calculation of the complete surface energy balance and that considers the respective prognostic variables of the RCM.

The setup and the testing of the RCM–MBM interface for two glaciers of the Swiss mass balance will be presented in Part II.

Acknowledgments. This study received financial support from a grant by the Swiss National Science Foundation (Grant 21-105214/1), the EU-funded action COST 719 (BBW C001.0041), and the International Max Planck Research School on Earth System Modelling (IMPRS-ESM). We thank Thomas Bosshard for his support in data analysis and four anonymous reviewers for their helpful and constructive comments.

REFERENCES

Arnold, N. S., I. C. Willis, M. J. Sharp, K. S. Richards, and W. J. Lawson, 1996: A distributed surface energy-balance model for a small valley glacier. I. Development and testing for Haut Glacier d'Arolla, Valais, Switzerland. *J. Glaciol.,* **42,** 77–89.

Brock, B. W., I. C. Willis, M. J. Sharp, and N. S. Arnold, 2000: Modelling seasonal and spatial variations in the surface energy balance of Haut Glacier d'Arolla, Switzerland. *Ann. Glaciol.,* **31,** 53–62.

Christensen, J. H., and O. B. Christensen, 2007: A summary of the PRUDENCE model projections of changes in European climate by the end of this century. *Climatic Change,* **81,** 7–30.

——, T. R. Carter, M. Rummukainen, and G. Amanatidis, 2007: Evaluating the performance and utility of regional climate models: The PRUDENCE project. *Climatic Change,* **81,** 1–6.

——, F. Boberg, O. B. Christensen, and P. Lucas-Picher, 2008: On the need for bias correction of regional climate change projections of temperature and precipitation. *Geophys. Res. Lett.,* **35,** L20709, doi:10.1029/2008GL035694.

Davies, H. C., 1976: A lateral boundary formulation for multi-level prediction models. *Quart. J. Roy. Meteor. Soc.,* **102,** 405–418.

Déqué, M., and Coauthors, 2005: Global high resolution versus Limited Area Model climate change projections over Europe: Quantifying confidence level from PRUDENCE results. *Climate Dyn.,* **25,** 653–670.

Efthymiadis, D., P. Jones, K. Briffa, I. Auer, R. Böhm, W. Schöner, C. Frei, and J. Schmidli, 2006: Construction of a 10-min-gridded precipitation data set for the Greater Alpine Region for 1800-2003. *J. Geophys. Res.,* **111,** D01105, doi:10.1029/2005JD006120.

Forland, E. J., and B. Aune, 1985: Comparison of Nordic methods for point precipitation correction. *Correction of Precipitation Measurements,* Zürcher Geographische Schriften 23, B. Sevruk, Ed., Geographisches Institut ETH Zürich, 239–244.

Frei, C., J. H. Christensen, M. Déqué, D. Jacob, R. G. Jones, and P. L. Vidale, 2003: Daily precipitation statistics in regional climate models: Evaluation and intercomparison for the European Alps. *J. Geophys. Res.,* **108,** 4124, doi:10.1029/2002JD002287.

Früh, B., J. W. Schipper, A. Pfeiffer, and V. Wirth, 2006: A pragmatic approach for downscaling precipitation in alpine-scale complex terrain. *Meteor. Z.,* **15,** 631–646.

Gaßmann, A., 2002: Numerische Verfahren in der nichthydrostatischen Modellierung und ihr Einfluss auf die Güte der Niederschlagsvorhersage (Numerical methods in nonhydrostatic modelling and their influence on the quality of the precipitation forecast). Ph.D. thesis, University of Bonn, 91 pp.

Giorgi, F., 1990: Simulation of regional climate using a limited area model nested in a general circulation model. *J. Climate,* **3,** 941–963.

Göttel, H., 2009: Einfluss der nichthydrostatischen Modellierung und der Niederschlagsverdriftung auf die Ergebnisse regionaler Klimamodellierung (Influence of nonhydrostatic modelling and precipitation drift on regional climate model results). Ph.D. thesis, University of Hamburg/Max Planck Institute for Meteorology, Hamburg, Germany, 126 pp.

Haeberli, W., and M. Hoelzle, 1995: Application of inventory data for estimating characteristics of and regional climate-change effects on mountain glaciers: A pilot study with the European Alps. *Ann. Glaciol.,* **21,** 206–212.

Hewitt, C., 2005: The ENSEMBLES Project—Providing ensemble-based predictions of climate changes and their impacts. *EGGS Newsl.,* **13,** 22–25.

Hock, R., 1999: A distributed temperature-index ice- and snowmelt model including potential direct solar radiation. *J. Glaciol.,* **45,** 101–111.

Jacob, D., 2001: A note to the simulation of the annual and inter-annual variability of the water budget over the Baltic Sea drainage basin. *Meteor. Atmos. Phys.,* **77,** 61–73.

——, and R. Podzun, 1997: Sensitivity studies with the regional climate model REMO. *Meteor. Atmos. Phys.,* **63,** 119–129.

——, and Coauthors, 2001: A comprehensive model inter-comparison study investigating the water budget during the BALTEX-PIDCAP period. *Meteor. Atmos. Phys.,* **77,** 19–43.

——, and Coauthors, 2007: An inter-comparison of regional climate models for Europe: Model performance in present-day climate. *Climatic Change,* **81,** 31–52.

Klok, E. J., and J. Oerlemans, 2002: Model study of the spatial distribution of the energy and mass balance of Morteratschgletscher, Switzerland. *J. Glaciol.,* **48,** 505–518.

Kotlarski, S., 2007: A subgrid glacier parameterisation for use in regional climate modelling. Ph.D. thesis, Reports on Earth System Science, Rep. 42, Max Planck Institute for Meteorology, Hamburg, Germany, 199 pp. [Available online at http://www.mpimet.mpg.de/fileadmin/publikationen/Reports/WEB_BzE_42.pdf.]

——, A. Block, U. Böhm, D. Jacob, K. Keuler, R. Knoche, D. Rechid, and A. Walter, 2005: Regional climate model simulations as input for hydrological applications: Evaluation of uncertainties. *Adv. Geosci.,* **5,** 119–125.

Machguth, H., F. Paul, M. Hoelzle, and W. Haeberli, 2006: Distributed glacier mass-balance modelling as an important component of modern multi-level glacier monitoring. *Ann. Glaciol.,* **43,** 335–343.

Majewski, D., 1991: *The Europa-Modell of the Deutscher Wetterdienst.* Vol. 2, *ECMWF Seminar on Numerical Methods in Atmospheric Models,* ECMWF, 147–191.

McGregor, J. L., 1997: Regional Climate Modelling. *Meteor. Atmos. Phys.,* **63,** 105–117.

Mitchell, T. D., T. R. Carter, P. D. Jones, M. Hulme, and M. New, 2004: A comprehensive set of high-resolution grids of monthly climate for Europe and the globe: The observed record (1901-2000) and 16 scenarios (2001-2100). Tyndall Centre Working Paper No. 55, Tyndall Centre for Climate Change Research, 30 pp.

New, M., M. Hulme, and P. Jones, 2000: Representing twentieth-century space–time climate variability. Part II: Development of 1901–96 monthly grids of terrestrial surface climate. *J. Climate,* **13,** 2217–2238.

Oerlemans, J., 2001: *Glaciers and Climate Change*. A. A. Balkema, 148 pp.

Paul, F., and S. Kotlarski, 2010: Forcing a distributed glacier mass balance model with the regional climate model REMO. Part II: Downscaling strategy and results for two Swiss glaciers. *J. Climate,* **23,** 1607–1620.

——, A. Kääb, M. Maisch, T. Kellenberger, and W. Haeberli, 2004: Rapid disintegration of Alpine glaciers observed with satellite data. *Geophys. Res. Lett.,* **31,** L21402, doi:10.1029/2004GL020816.

Radić, V., and R. Hock, 2006: Modeling future glacier mass balance and volume changes using ERA-40 reanalysis and climate models: A sensitivity study at Storglaciären, Sweden. *J. Geophys. Res.,* **111,** F03003, doi:10.1029/2005JF000440.

Raper, S. C. B., and R. J. Braithwaite, 2006: Low sea level rise projections from mountain glaciers and icecaps under global warming. *Nature,* **439,** 311–313.

Reichert, B. K., L. Bengtsson, and J. Oerlemans, 2002: Recent glacier retreat exceeds internal variability. *J. Climate,* **15,** 3069–3081.

Roe, G. H., 2005: Orographic precipitation. *Annu. Rev. Earth Planet. Sci.,* **33,** 645–671.

Roeckner, E., and Coauthors, 1996: The atmospheric general circulation model ECHAM-4: Model description and simulation of present-day climate. Rep. 218, Max Planck Institute for Meteorology, Hamburg, Germany, 90 pp.

Schneeberger, C., O. Albrecht, H. Blatter, M. Wild, and R. Hock, 2001: Modelling the response of glaciers to a doubling in atmospheric CO_2: A case study of Storglaciären, northern Sweden. *Climate Dyn.,* **17,** 825–834.

Schwarb, M., 2000: The Alpine precipitation climate—Evaluation of a high-resolution analysis scheme using comprehensive rain-gauge data. Ph.D. thesis, Swiss Federal Institute of Technology, Zurich, Switzerland, 131 pp.

Semmler, T., and D. Jacob, 2004: Modeling extreme precipitation events—A climate change simulation for Europe. *Global Planet. Change,* **44,** 119–127.

Sevruk, B., 1982: Methods of correction for systematic errors in point precipitation measurement for operational use. WMO Hydrol. Rep. 21, WMO 589, WMO, 91 pp.

Simmons, A. J., and D. M. Burridge, 1981: An energy and angular-momentum conserving vertical finite-difference scheme and hybrid vertical coordinate. *Mon. Wea. Rev.,* **109,** 758–766.

Stahl, K., R. D. Moore, J. M. Shea, D. Hutchinson, and A. J. Cannon, 2008: Coupled modelling of glacier and streamflow response to future climate scenarios. *Water Resour. Res.,* **44,** W02422, doi:10.1029/2007WR005956.

Uppala, S. M., and Coauthors, 2005: The ERA-40 Re-Analysis. *Quart. J. Roy. Meteor. Soc.,* **131,** 2961–3012.

Van de Wal, R. S. W., and M. Wild, 2001: Modelling the response of glaciers to climate change by applying volume-area scaling in

combination with a high resolution GCM. *Climate Dyn.,* **18,** 359–366.

WGMS, 1989: World glacier inventory—Status 1988. W. Haeberli et al., Eds., World Glacier Monitoring Service, 458 pp.

——, 2008: Global glacier changes: Facts and figures. M. Zemp et al., Eds., World Glacier Monitoring Service, 88 pp.

Widmann, M., C. S. Bretherton, and E. P. Salathé Jr., 2003: Statistical precipitation downscaling over the northwestern United States using numerically simulated precipitation as a predictor. *J. Climate,* **16,** 799–816.

Wilby, R. L., L. E. Hay, W. J. Gutowski Jr., R. W. Arritt, E. S. Takle, Z. Pan, G. Leavesley, and M. P. Clark, 2000: Hydrological responses to dynamically and statistically downscaled climate model output. *Geophys. Res. Lett.,* **27,** 1199–1202.

Zemp, M., M. Hoelzle, and W. Haeberli, 2007: Distributed modelling of the regional climatic equilibrium line altitude of glaciers in the European Alps. *Global Planet. Change,* **56,** 83–100.

——, F. Paul, M. Hoelzle, and W. Haeberli, 2008: Glacier fluctuations in the European Alps 1850–2000: An overview and spatio-temporal analysis of available data. *The Darkening Peaks: Glacial Retreat in Scientific and Social Context,* B. Orlove, E. Wiegandt, and B. Luckman, Eds., University of California Press, 152–167.